

# Hydrogen Bonding and Proton Transfers Involving Triply Bonded Atoms. $\text{HC}\equiv\text{CH}$ and $\text{HC}\equiv\text{N}$

Slawomir M. Cybulski and Steve Scheiner\*†

Contribution from the Department of Chemistry & Biochemistry, Southern Illinois University, Carbondale, Illinois 62901. Received January 7, 1987

**Abstract:** The formation of the H-bonded complexes  $(\text{HCCH}\cdots\text{CCH})^-$ ,  $(\text{NCH}\cdots\text{CN})^-$ ,  $(\text{CNH}\cdots\text{NC})^-$ ,  $(\text{NCH}\cdots\text{NC})^-$ , and  $(\text{CNH}\cdots\text{CN})^-$  and the subsequent proton transfers taking place within them are studied by ab initio methods. When all H bonds are constrained to the same length, the proton-transfer barrier diminishes as the acceptor group becomes more basic. Hence, the "intrinsic" barrier for proton transfer between C atoms is lower than that for internitrogen transfer. However, greater acidity of the proton donor group leads to a stronger and hence shorter H bond in which the proton needs to traverse a smaller distance from donor to acceptor. Consequently, when the length of the H bond is freed of external restraint, the dominant factor controlling the height of the transfer barrier switches from the acceptor to the donor group. While the full potential energy surface characterizing proton transfer between C atoms contains a pair of equivalent minima separated by an energy barrier, internitrogen transfer occurs in the absence of a barrier. Only one minimum, corresponding to  $(\text{NCH}\cdots\text{NC})^-$ , is present in the potential of the asymmetric system. These principles explain the previously observed difference in proton transfer behavior between C acids and normal acids containing N and O atoms.

It has been pointed out on numerous occasions<sup>1-4</sup> that proton transfer between C atoms is fundamentally rather different than the same process involving electronegative atoms like N or O. Whereas Brønsted plots of proton transfers in the latter case are generally sharply curved, the rate is very nearly a linear function of the overall exothermicity of the transfer reaction involving C atoms over a  $\text{p}K$  range as large as 10 units.<sup>4</sup> This finding, in conjunction with the much slower proton transfer rates observed for C bases, has led to the general conclusion that the intrinsic energy barrier for transfer between C atoms is much higher than that for the electronegative atoms, in the gas phase as well as in solution.<sup>4</sup> Among the various reasons hypothesized for this difference have been changes in electron delocalization and hybridization accompanied by geometry alterations, poor H-bonding characteristics of C, and solvent reorganization in the transition state.<sup>3</sup>

An unequivocal understanding of the different behavior of C would be of great fundamental interest. It is to this end that ab initio molecular orbital techniques may be applied to great advantage. Such a quantum mechanical approach is ideally suited to analysis of intrinsic properties without the complexities introduced by the presence of solvent. It is possible to obtain accurate information concerning molecular geometries and their electronic structure. Unfortunately, in contrast to the substantial degree of prior theoretical attention to proton transfers within H bonds involving electronegative atoms, the C analogues have been relatively ignored. Moreover, the small number of calculations of the latter systems<sup>5-8</sup> have generally been less than reliable due to use of small, unpolarized basis sets and neglect of electron correlation.

Perhaps the most obvious difference between carbon acids and those containing more electronegative elements is the much weaker proton donating ability of the former. If one wishes to uncover any additional factors that contribute to the uniqueness of intercarbon proton transfer, this overriding difference must first be ameliorated by investigating C acids that are as strongly proton donating as possible. The intrinsically strongest carbon acids are those involving  $\text{sp}$  hybridization within a triple bond. For example, there is recent evidence<sup>9</sup> that this sort of hybridization makes a simple alkyne like  $\text{HC}\equiv\text{CH}$  comparable in gas-phase acidity to an alkane that has been trifluoro substituted ( $\text{CF}_3\text{H}$ ). As our first model system, we therefore choose the proton transfer between C atoms in  $(\text{HC}\equiv\text{CH}\cdots\text{C}\equiv\text{CH})^-$ .

HCN also involves a triply bonded C atom and should nicely bridge the gap between C and the electronegative atoms since, as noted by Bednar and Jencks, HCN is the most normal carbon acid known while retaining behavior characteristic of other carbon

acids.<sup>3</sup> Extending our study to HCN also offers some interesting additional opportunities. First of all, since HCN is somewhat more acidic than HCCH, we may examine the manner in which the proton-transfer process is affected by this parameter without tampering with the C hybridization. Second, the N end of  $\text{C}\equiv\text{N}^-$  is also capable of being protonated, although less readily (see below). We may thus directly compare the proton transfer properties of C with N on the same species. Hence, in addition to  $(\text{HC}\equiv\text{CH}\cdots\text{C}\equiv\text{CH})^-$ , we also examine proton transfers between  $\text{CN}^-$  anions:  $(\text{N}\equiv\text{CH}\cdots\text{C}\equiv\text{N})^-$ ,  $(\text{C}\equiv\text{NH}\cdots\text{N}\equiv\text{C})^-$ , and  $(\text{N}\equiv\text{CH}\cdots\text{N}\equiv\text{C})^-$ . The latter asymmetric system is especially relevant since proton transfer from C to N has been demonstrated to proceed through a H-bonded intermediate.<sup>10</sup> A further benefit of the use of these simple models in the gas phase is that some of the factors suggested earlier for the different behavior of carbon acids, such as solvent reorganization or geometry changes induced by rehybridization, can immediately be ruled out, focussing our attention on the remaining possibilities.

After a brief discussion of our theoretical method and the reasons for its choice, the calculated energetics of formation of the various complexes and the barriers for the proton transfers within them are compared. The rates of these transfers are then computed, including the influence of isotopic substitution, and analyzed as to the relative contribution of tunneling over a wide range of temperature. Finally, the energetics of proton transfer are compared under the condition of uniform H-bond lengths in all systems.

(1) Eigen, M. *Angew. Chem., Int. Ed. Engl.* **1964**, *3*, 1. Bell, R. P. *The Proton in Chemistry*; Cornell University Press: Ithaca, NY, 1973. Jones, J. R. *The Ionization of Carbon Acids*; Academic Press: New York, 1973.

(2) Kresge, A. J. *Acc. Chem. Res.* **1975**, *8*, 354. Koch, H. F. *Ibid.* **1984**, *17*, 137. Ritchie, C. D. *J. Am. Chem. Soc.* **1969**, *91*, 6479. Bordwell, R. G.; Boyle, W. J., Jr. *Ibid.* **1975**, *97*, 3447. Streitwieser, A., Jr.; Holtz, D.; Zeigler, G. R.; Stoffer, J. O.; Brokaw, M. L.; Guibe, F. *Ibid.* **1976**, *98*, 5229. Bernasconi, C. F.; Hibdon, S. A.; McMurry, S. E. *Ibid.* **1982**, *104*, 3459.

(3) Bednar, R. A.; Jencks, W. P. *J. Am. Chem. Soc.* **1985**, *107*, 7117, 7126, 7135.

(4) Han, C.-C.; Dodd, J. A.; Brauman, J. I. *J. Phys. Chem.* **1986**, *90*, 471. Farneth, W. E.; Brauman, J. I. *J. Am. Chem. Soc.* **1976**, *98*, 7891.

(5) Cao, H. Z.; Allavena, M.; Tapia, O.; Evleth, E. M. *J. Phys. Chem.* **1985**, *89*, 1581; *Chem. Phys. Lett.* **1983**, *96*, 458.

(6) Bertran, J.; Lledos, A. *J. Mol. Struct. (Theochem)* **1985**, *123*, 211.

(7) Jones, W. H.; Mariani, R. D.; Lively, M. L. *Chem. Phys. Lett.* **1984**, *108*, 602. Jones, W. H.; Mezey, P. G.; Csizmadia, I. G. *J. Mol. Struct. (Theochem)* **1985**, *121*, 85.

(8) Alagona, G.; Desmeules, P.; Ghio, C.; Kollman, P. A. *J. Am. Chem. Soc.* **1984**, *106*, 3623.

(9) Fraser, G. T.; Lovas, F. J.; Suenram, R. D.; Nelson, D. D., Jr.; Klemperer, W. J. *Chem. Phys.* **1986**, *84*, 5983.

(10) Meot-Ner, M. *J. Am. Chem. Soc.* **1979**, *101*, 2389. Attina, M.; Cacace, F.; Giacomello, P.; Speranza, M. *Ibid.* **1980**, *102*, 6896. Moylan, C. R.; Brauman, J. I. *Ibid.* **1985**, *107*, 761.

\* Recipient of NIH Research Career Development Award.

**Table I.** Deprotonation Energies (kcal/mol) with and without BSSE Corrections

	MP2/ 6-31+G**		SCF/ 6-31+G**		SCF/4-31G		exptl <sup>a</sup>
	corr	uncorr	corr	uncorr	corr	uncorr	
	HCCH	380.3	381.7	384.8	385.1	402.5	
HCN	350.9	352.5	353.4	353.9	367.3	374.2	355.7
HNC	332.9	335.0	342.2	343.0	361.6	364.7	

<sup>a</sup>Evaluated by subtracting  $\frac{5}{2}RT$  ( $\Delta pV$  + translational correction) from  $\Delta H^\circ(298\text{ K})^{25}$  and adding change in zero-point vibrational energy evaluated from SCF/6-31+G\*\* force constants (Table V).

### Selection of Theoretical Method

All calculations were carried out with the ab initio GAUSSIAN-80 package of computer codes.<sup>11</sup> The primary basis set used was 6-31+G\*\* which contains polarization functions,<sup>12</sup> d for C and N and p for H ( $\alpha_p = 0.15$ ), on all centers as well as a diffuse sp set on all C and N atoms.<sup>13</sup> The effects of electron correlation were included by way of second-order Møller–Plesset perturbation theory (MP2).<sup>14,15</sup> Also tested, for purposes of comparison, was the unpolarized 4-31G set.<sup>16</sup> Full geometry optimizations were carried out with the gradient schemes contained within the program. Vibrational frequencies were calculated from SCF/6-31+G\*\* force constants by the standard FG matrix operation,<sup>17</sup> using a locally written code. The counterpoise procedure of Boys and Bernardi<sup>18</sup> was used to evaluate corrections for the basis set superposition error (BSSE) at the SCF and MP2 levels, as recommended by numerous workers.<sup>19–24</sup>

In order for the energetics of proton transfer to be treated properly, it is essential that the theoretical method accurately reflect the intrinsic proton affinity of each subunit. The energy

required to remove a proton from a given molecule HA was computed as the difference in total energy between HA and its deprotonated anion A<sup>-</sup>, with the geometries of both species fully optimized at the SCF level. These deprotonation energies are reported in Table I for three different levels of theory. In each case, it is possible to correct the value for BSSE by the counterpoise procedure.

The SCF/4-31G values are all rather high, not surprising when calculating the proton affinities of anions which typically require much more flexible basis sets. In confirmation of this notion, the superposition errors are quite large for 4-31G, lying in the range between 3 and 7 kcal/mol. The BSSE is an order of magnitude smaller for the 6-31+G\*\* set, which also leads to much lower deprotonation energies at the SCF level. A further reduction results from inclusion of correlation at the second order of perturbation theory, as seen in the first columns of the table. This diminution of the deprotonation energy varies from 2.5 kcal/mol for HCN to 9.3 for HNC; hence, correlation plays a key role in the relative proton affinities of the two ends of CN<sup>-</sup>.

Comparison with the last column of the table indicates that our 6-31+G\*\* basis set is capable of reproducing experimental deprotonation energies<sup>25</sup> rather well. The SCF values are within 2 kcal/mol of experiment although the errors for HCCH and HCN are in opposite directions. This trend is not particular to the 6-31+G\*\* set but is characteristic also of much larger basis sets, even those approaching the Hartree–Fock limit.<sup>26</sup> Inclusion of second-order correlation leads to a small and uniform underestimation of experimental values.

In the latter context, it should be pointed out that since the zero-point vibrational corrections to the experimental data were calculated at the SCF level, which is well-known to exaggerate the true frequencies, the “experimental” values in the last column are probably likewise overestimated. In fact, recent calculations by Ewig and Van Wazer<sup>27</sup> have shown that correlation reduces the contribution of the zero-point vibrations to the deprotonation energy of HCN by some 10%. For the same molecule, they found that retaining the perturbation expansion up to the MP4 level increases the deprotonation energy by 2.6 kcal/mol. The same authors tested the effect of optimizing geometries at the MP2 rather than the SCF level and found only a very minimal change in their computed deprotonation energy. Hence, the bulk of the discrepancy between the experimental and calculated deprotonation energies in Table I could probably be removed by a more complete treatment of correlation, coupled with more accurate force constants. In sum, the MP2/6-31+G\*\* procedure appears to provide a well-balanced and cost-effective treatment of the relevant systems, with lingering errors of small magnitude and of uniform nature from one system to the next.

At our highest level of theory, MP2/6-31+G\*\* corrected for BSSE, the deprotonation energy of HCN is higher by 18.0 kcal/mol than that of HNC. Neglect of correlation lowers the difference in energy between HCN and HNC to 11.2 kcal/mol, thereby exaggerating the tendency of the proton to be attracted toward the N end of CN<sup>-</sup>. This problem is more severe with 4-31G for which the difference in energy between HCN and HNC is only 5.7 kcal/mol. The magnitude of the energetic preference of a proton for the C atom of CN<sup>-</sup> is emphasized here because it has important ramifications upon the calculated results below. Parenthetically, it is interesting that the greater ease of removing a proton from the N end of the molecule persists into the protonated cations as well, as indicated by the smaller deprotonation energies of RCNH<sup>+</sup> as compared to RNCH<sup>+</sup>.<sup>28</sup>

### Energetics

**Geometries.** The geometries of all species were optimized at the SCF level with both the 6-31+G\*\* and 4-31G basis sets and

(11) Binkley, J. S.; Whiteside, R. A.; Krishnan, R.; Seeger, R.; DeFrees, D. J.; Schlegel, H. B.; Topiol, S.; Kahn, L. R.; Pople, J. A. *QCPE* 1981, 406.

(12) Hariharan, P. C.; Pople, J. A. *Theor. Chim. Acta* 1973, 28, 213. Chandrasekhar, J.; Andrade, J. G.; Schleyer, P. v. R. *J. Am. Chem. Soc.* 1981, 103, 5609.

(13) In the case of complexes of HCCH with CCH<sup>-</sup>, use of the standard diffuse orbital exponent of 0.04 for C led to numerical instabilities in the SCF procedure. This problem was avoided by raising this exponent to 0.07 in all systems involving HCCH.

(14) Møller, C.; Plesset, M. S. *Phys. Rev.* 1934, 46, 618. Binkley, J. S.; Pople, J. A. *Int. J. Quantum Chem.* 1975, 9, 229.

(15) Due to an excessive number of atomic orbitals and to numerical instabilities requiring greater precision, MP2 calculations for the (HCCH<sup>-</sup>·CCH<sup>-</sup>) system were carried out at the San Diego Supercomputer Center with the Cray version of GAUSSIAN-82: Binkley, J. S.; Frisch, M. J.; Raghavachari, K.; DeFrees, D. J.; Schlegel, H. B.; Whiteside, R. A.; Fluder, E. M.; Seeger, R.; Pople, J. A. GAUSSIAN82, Carnegie-Mellon University: Pittsburgh, PA, 1982.

(16) Ditchfield, R.; Hehre, W. J.; Pople, J. A. *J. Chem. Phys.* 1971, 54, 724.

(17) Wilson, E. B., Jr.; Decius, J. C.; Cross, P. C. *Molecular Vibrations*; Dover, NY, 1955.

(18) Boys, S. F.; Bernardi, F. *Mol. Phys.* 1970, 19, 553.

(19) Zahradnik, R.; Hobza, P. *Int. J. Quantum Chem.* 1986, 29, 663. Hobza, P.; Schneider, B.; Carsky, P.; Zahradnik, R. *J. Mol. Struct. (Theor. Chem)* 1986, 138, 377. Hobza, P.; Mehlhorn, A.; Carsky, P.; Zahradnik, R. *Ibid.* 1986, 138, 387.

(20) van Lenthe, J. H.; van Duijneveldt-van de Rijdt, J. G. C. M.; van Duijneveldt, F. B. *Adv. Chem. Phys.* Lawley, K., Ed., in press. Chalasinski, G.; Gutowski, M. *Mol. Phys.* 1986, 57, 427. Gutowski, M.; van Lenthe, J. H.; Verbeek, J.; van Duijneveldt, F. B.; Chalasinski, G. *Chem. Phys. Lett.* 1986, 124, 370. Bulski, M.; Chalasinski, G. *Ibid.* 1986, 128, 25. Gutowski, M.; van Duijneveldt, F. B.; Chalasinski, G.; Piela, L. *Ibid.* 1986, 129, 325.

(21) Cole, S. J.; Szalewicz, K.; Purvis, G. D., III; Bartlett, R. J. *J. Chem. Phys.* 1986, 84, 6833. Cole, S. J.; Szalewicz, K.; Bartlett, R. J. *Int. J. Quantum Chem.* 1986, 30, 695.

(22) (a) Burton, P. G.; Senff, U. E. *J. Chem. Phys.* 1982, 76, 6073. (b) Meyer, W.; Hariharan, P. C.; Kutzelnigg, W. *Ibid.* 1980, 73, 1880. (c) Szczesniak, M. M.; Scheiner, S. *Ibid.* 1986, 84, 6328. (d) Leclercq, J. M.; Allavena, M.; Bouteiller, Y. *Ibid.* 1983, 78, 4606.

(23) Cammi, R.; Bonaccorsi, R.; Tomasi, J. *Theor. Chim. Acta* 1985, 68, 271. Bonaccorsi, R.; Cammi, R.; Tomasi, J. *Int. J. Quantum Chem.* 1986, 29, 373.

(24) Kolos, W. *Theor. Chim. Acta* 1980, 54, 187; 1979, 51, 219. Kurdi, L.; Kochanski, E.; Diercksen, G. H. F. *Chem. Phys.* 1985, 92, 287. Mathers, T. L.; Kestner, N. R. *Int. J. Quantum Chem. QCS* 1986, 19, 297. Rendell, A. P. L.; Bacskay, G. B.; Hush, N. S. *Chem. Phys. Lett.* 1985, 117, 400. Wells, B. H.; Wilson, S. *Mol. Phys.* 1986, 57, 421. Roszak, S.; Sokalski, W. A.; Hariharan, P. C.; Kaufman, J. J. *Theor. Chim. Acta* 1986, 70, 81. Bachrach, S. M.; Streitwieser, A., Jr. *J. Am. Chem. Soc.* 1984, 106, 2283.

(25) Bartmess, J. E.; McIver, R. T., Jr. In *Gas Phase Ion Chemistry*; Bowers, M. T., Ed.; Academic Press: New York, 1979; Vol. 2, Chapter 11.

(26) Lee, T. J.; Schaefer, H. F., III *J. Chem. Phys.* 1985, 83, 1784.

(27) Ewig, C. S.; Van Wazer, J. R. *J. Phys. Chem.* 1986, 90, 4360.

(28) Meot-Ner, M.; Karpas, Z.; Deakne, C. A. *J. Am. Chem. Soc.* 1986, 108, 3913.

**Table II.** Optimized Bond Lengths (Å) and SCF Energies (au)<sup>a</sup>

	6-31+G**	4-31G	6-31+G**	4-31G
H—C≡C—H				
H—C	1.058	1.051	1.061	1.057
C≡C	1.188	1.190	1.231	1.234
E	-76.8233	-76.7114	-76.2096	-76.0608
H—C≡N				
H—C	1.060	1.051		
C≡N	1.133	1.140	1.162	1.170
E	-92.8782	-92.7319	-92.3142	-92.1356
H—N≡C				
H—C	0.987	0.979		
N≡C	1.154	1.162	0.987	0.979
E	-92.8608	-92.7168		
(HC≡C—H...C≡CH) <sup>-</sup>				
H—C	1.057	1.050	1.059	1.053
C≡C	1.193	1.197	1.213	1.213
C—H	1.082	1.095	1.405	1.399
C...C	3.354	3.164	2.809	2.798
C≡C	1.227	1.226	1.213	1.213
C—H	1.061	1.055	1.059	1.053
E	-153.0491	-152.7991	-153.0282	-152.7864
(N≡C—H...C≡N) <sup>-</sup>				
N≡C	1.138	1.145	1.149	1.155
C—H	1.091	1.105	1.393	1.382
C...C	3.201	3.033	2.787	2.765
C≡N	1.158	1.162	1.149	1.155
E	-185.2234	-184.9124	-185.2084	-184.9037
(C≡N—H...N≡C) <sup>-</sup>				
C≡N	1.150	1.160	1.155	1.164
N—H	1.041	1.072	1.259	1.256
N...N	2.754	2.631	2.519	2.513
N≡C	1.159	1.166	1.155	1.164
E	-185.2161	-184.9039	-185.2106	-184.9019
(N≡C—H...N≡C) <sup>-</sup>				
N≡C	1.138	1.146	1.150	1.155
C—H	1.090	1.108	1.431	1.417
C...N	3.011	2.858	2.657	2.642
N≡C	1.160	1.168	1.155	1.164
E	-185.2266	-184.9115	-185.2090	-184.9028
(C≡N—H...C≡N) <sup>-</sup>				
C≡N	1.150	1.160	1.155	1.164
N—H	1.045	1.069	1.226	1.225
N...C	2.907	2.787	2.657	2.642
C≡N	1.156	1.160	1.150	1.155
E	-185.2133	-184.9046	-185.2090	-184.9028

<sup>a</sup> Bonds of each system are listed in order from left to right.

the results are reported in Table II, along with the SCF energy. Following the monomer geometries in the upper portion of the table, the complexes on the left side correspond to minima in the potential energy surfaces while those on the right represent transition states to proton transfer. All geometries are linear: the transition states belong to the  $D_{\infty h}$  point group with the exception of  $(N\equiv C\cdots H\cdots N\equiv C)^-$  which is  $C_{\infty v}$  as are the various equilibrium complexes. The order in which the bond lengths are listed in Table II corresponds to a left  $\rightarrow$  right direction within the system.

Beginning our analysis with the monomers in the upper portion of Table II, there is a general trend for the larger basis set to predict shorter triple bonds than does 4-31G (particularly for  $C\equiv N$ ) as well as longer C—H and N—H bonds. Both basis sets indicate a substantially longer  $C\equiv N$  bond in HNC than in HCN. Also, the triple bond undergoes a noticeable stretch upon deprotonation of any of the monomers. Upon complexation, the H-bonding proton is pulled toward the anion, elongating the corresponding X—H bond. This elongation is more pronounced with the 4-31G basis set which also leads to substantially shorter intermolecular distances, due in part to the greater BSSE associated with this basis. Comparison of the geometries of the complexes with the transition states on their right shows a clear trend for reduction in the intermolecular separation as the proton is being transferred. These contractions range from 0.235 Å for

**Table III.** Binding Energies of Various Complexes (kcal/mol) with and without BSSE Corrections

	MP2/ 6-31+G**		SCF/ 6-31+G**		SCF/4-31G	
	corr	uncorr	corr	uncorr	corr	uncorr
$(HCCH\cdots CCH)^-$	10.8	12.0	9.8	10.2	12.0	16.9
$(NCH\cdots CN)^-$	19.5	20.7	18.9	19.5	21.6	28.1
$(NCH\cdots NC)^-$	20.0	22.1	20.6	21.4	24.7	27.6
$(CNH\cdots CN)^-$	27.4	29.5	23.0	24.0	25.6	32.8
$(CNH\cdots NC)^-$	27.5	30.3	24.5	25.8	28.8	32.3

$(C\equiv N—H\cdots N\equiv C)^-$  to 0.545 Å for  $(HC\equiv C—H\cdots C\equiv CH)^-$ , calculated with our larger basis set.

**Binding Energies.** The binding energy of each complex is defined as the difference in total energy between the complex on one hand and the isolated subsystems of which it is composed on the other. The SCF/4-31G binding energies listed in Table III pertain to geometries optimized with that basis set and 6-31+G\*\* values to structures optimized at the SCF/6-31+G\*\* level. MP2/6-31+G\*\* data were derived from SCF geometries; the accuracy of this approximation was checked as described below. For each level of theory, the results are reported both before and after BSSE corrections have been included.

The binding energy of HCCH with  $CCH^-$  is calculated to be 10.8 kcal/mol with our most accurate corrected MP2/6-31+G\*\* approach. In contrast, the binding of  $CN^-$  to HCN or HNC is approximately twice as strong, with interaction energies in the range between 19.5 and 27.5 kcal/mol. The binding energy appears to be quite insensitive to the specific atom of  $CN^-$  which is donating the electrons: When HCN acts as proton donor, the binding energies are around 20 kcal/mol regardless of whether  $CN^-$  interacts with the proton via its C or N end. The same is true for HNC as proton donor, with a somewhat higher binding energy of 27.5 kcal/mol. These trends are generally supported by the lower levels of theory, although perhaps not as precisely.

Within the subset of symmetrical systems, the binding energies clearly increase in the following order at any level of theory:



This pattern is consistent with the experimentally observed trend<sup>29</sup> of an inverse correlation between the proton affinity of B and the binding energy of a symmetric proton-bound complex of the type  $(BH-B)^+$ .

Correlation is responsible for 1.0 kcal/mol of the total binding energy of  $(HCCH\cdots CCH)^-$  since the interaction energy is reduced by this amount to 9.8 kcal/mol at the SCF/6-31+G\*\* level. The influence of electron correlation is somewhat smaller when HCN acts as proton donor. The corrected MP2/6-31+G\*\* binding energy of  $(NCH\cdots CN)^-$  is only 0.6 kcal/mol greater than the SCF value while a decrease of like amount is noted for  $(NCH\cdots NC)^-$ . In contrast, correlation is responsible for substantial increases in the binding energies of both complexes in which HNC acts as proton donor. This difference in behavior may be traced to the influence of correlation upon the dipole moment of the two molecules. Whereas the MP2 moment of HCN is smaller than the SCF value (by 0.36 D), correlation *increases* the moment of HNC by 0.27 D. The reduced moment in HCN destabilizes the complex by lowering the electrostatic interaction with the partner anion.<sup>22c</sup> This correlation-induced destabilization is counteracted in large measure by the attractive dispersion energy that is contained within the MP2 interaction.<sup>30</sup> As a result of cancellation between these two effects, the total MP2 contribution to the interaction energy in HCN complexes is quite small. On the other hand, the increase in the moment of HNC caused by correlation enhances the attraction, as does the dispersion; addition of these

(29) Hiraoka, K.; Takimoto, H.; Yamabe, S. *J. Phys. Chem.* **1986**, *90*, 5910.

(30) Szczesniak, M. M.; Latajka, Z.; Scheiner, S. *J. Mol. Struct. (Thechem)* **1986**, *135*, 179. Latajka, Z.; Scheiner, S. *J. Chem. Phys.* **1986**, *84*, 341. Szczesniak, M. M.; Scheiner, S. *Ibid.* **1985**, *83*, 1778. Latajka, Z.; Scheiner, S. *Ibid.* **1984**, *81*, 4014.

**Table IV.** Energy Barriers to Proton Transfer (kcal/mol) from Left to Right

	MP2/ 6-31+G**	SCF/ 6-31+G**	SCF/ 4-31G
(HCCH...CCH) <sup>-</sup>	7.6	13.1	8.0
(NCH...CN) <sup>-</sup>	5.3	9.5	5.4
(CNH...NC) <sup>-</sup>	0.0	3.4	1.3
(NCH...NC) <sup>-</sup>	8.4	11.0	5.5
(CNH...CN) <sup>-</sup>	-1.7	2.7	1.1

two factors leads to the large MP2 contributions in Table III.

A second pattern noted in Table III is the smaller contribution of correlation to binding energies when the CN<sup>-</sup> anion interacts with its partner through its N end. This weakened interaction at the MP2 level may be explained by a correlation-induced shift of electron density from N to C within CN<sup>-</sup> which lessens the electrostatic interaction of N with the partial positive charge on the H atom. This notion conforms to the previously mentioned effect of correlation in decreasing the proton affinity of the N end of CN<sup>-</sup> relative to the C end (Table I). Indeed, a shift of charge in this direction has in fact been recently observed by Fowler and Klein.<sup>31</sup> As a result of neglecting correlation, the SCF data exaggerate the sensitivity of the binding energies to the nature of the proton acceptor. The energetic distinction between the C and N ends of CN<sup>-</sup> as proton acceptor are less than 0.5 kcal/mol at the MP2/6-31+G\*\* level, 1.7 for SCF/6-31+G\*\*, and more than 3 kcal/mol for SCF/4-31G (all corrected for BSSE).

The 4-31G data are subject to quite large superposition errors, of a fairly erratic nature from one complex to the next. Failure to remove the BSSE would reverse the conclusion that the N end of CN<sup>-</sup> binds more strongly. After corrections are made for BSSE, the SCF/4-31G binding energies reproduce the qualitative trends reasonably well but remain in quantitative error. For example, while the corrected 4-31G binding energy of (CNH...CN)<sup>-</sup> is underestimated relative to the MP2/6-31+G\*\* value by 1.8 kcal/mol, the former approximate procedure overestimates this quantity for the remaining complexes by various amounts. The 6-31+G\*\* superposition errors are much smaller and fairly uniform from one complex to the next; hence, removal of BSSE is necessary only for quantitative accuracy.

As has been noted in the literature, SCF calculations, uncorrected for BSSE, can in certain instances yield results in reasonable agreement with much more accurate data. This agreement is due in large part to replacement of real correlation forces that are omitted at the SCF level by artificial attractive effects of basis set superposition. However, these two effects are only of equal magnitude in fortuitous circumstances and can certainly not be expected to quantitatively cancel one another over an extended region of configuration space. Within the context of systems studied here, we point out that with the coincidental exception of (NCH...CN)<sup>-</sup>, the artificial enhancement of the SCF binding energy produced by BSSE does *not* compensate for the true stabilization of the complex caused by correlation effects, as may be seen by a comparison of the first and fourth columns of data in Table III.

**Proton-Transfer Barriers.** The energy barriers to proton transfer reported in Table IV were calculated as the difference in energy between the complexes on the left side of Table II and the corresponding transition state on the right. For all systems investigated, the data corroborate a trend that has been noted on numerous occasions previously: the barrier is raised by an increase in the size of the basis set but is lowered by inclusion of electron correlation.<sup>32,33</sup>

Beginning with transfer between C atoms, comparison of the first two rows reveals a lower barrier for transfer between two NC<sup>-</sup> anions as compared to HCC<sup>-</sup> at all levels of theory. The

**Table V.** Zero-Point Vibrational Energies (kcal/mol) Calculated at SCF/6-31+G\*\* Level

	L = H	L = D		L = H	L = D
LCC <sup>-</sup>	9.85	8.13	(N≡C...L...C≡N) <sup>-</sup>	12.96	11.87
LCCL	18.41	14.62	(C≡N...L...N≡C) <sup>-</sup>	15.51	13.49
CN <sup>-</sup>	3.33	3.33	(C≡N...L...N≡C) <sup>-</sup>	12.87	11.70
LCN	11.22	9.34	(N≡C...L...N≡C) <sup>-</sup>	15.74	13.76
LNC	10.64	8.76	(N≡C...L...N≡C) <sup>-</sup>	12.92	11.79
(LC≡C...L...C≡CL) <sup>-</sup>	29.37	23.71	(C≡N...L...C≡N) <sup>-</sup>	15.52	13.53
(LC≡C...L...C≡CL) <sup>-</sup>	26.83	22.00	(C≡N...L...C≡N) <sup>-</sup>	12.92	11.79
(N≡C...L...C≡N) <sup>-</sup>	15.73	13.77			

barrier is dramatically reduced when the transfer takes place between two N atoms, as may be seen in the next row. Hence, given equivalent hybridization patterns (here sp), transfer between a pair of N atoms is more facile than for the less electronegative carbon analogues. This finding is consistent with experimental observation of proton-transfer behavior in solution<sup>1-3</sup> and falls in line with similar principles relating N to the more electronegative oxygen.<sup>33,34</sup>

A general rule covering all three symmetric systems is that smaller deprotonation energies of the neutral monomers lead to lower barriers to proton transfer in the corresponding complexes. In other words, the barrier is reduced as the proton donor molecule becomes more acidic. This finding is not a trivial one since the higher acidity of the proton donor molecule implies a lesser proton affinity of its conjugate base, acting as proton acceptor within the complex, which one might ordinarily associate with a *higher* barrier. We conclude that it is the identity of the proton donor and not the acceptor that is the key factor in the proton transfer barrier, just as was noted above for the binding energies.

With regard to the asymmetric (CN...H...CN)<sup>-</sup> system in the last two rows, transfer of a proton from C to N leads to a rather high barrier, easily explained by the endothermicity of this process, due to the much higher proton affinity of the C end of CN<sup>-</sup>. The barrier for the reverse direction of transfer is of course lower at all levels of theory. In fact, correlation stabilizes the (CN...H...CN)<sup>-</sup> configuration so much that it is lower in energy than (CNH...CN)<sup>-</sup>, explaining the negative MP2 entry in Table IV. This situation corresponds to the transition from an asymmetric double-well potential with a true barrier at the SCF level to an MP2 potential in which the only minimum is (CN...HCN)<sup>-</sup> (see below).

It is interesting to note that due to the opposing effects on the barrier of basis set enlargement and correlation, the SCF/4-31G barriers are surprisingly close to the corresponding MP2/6-31+G\*\* values for the symmetric systems in the first three rows. However, since 4-31G greatly underestimates the energy difference between HCN and HNC, it likewise underestimates the difficulty of transferring a proton from C to N within the (NCH...NC)<sup>-</sup> complex (i.e., low barrier). The barrier for the reverse direction is correspondingly overestimated with SCF/4-31G.

As noted above, the effects of correlation have been included by performing MP2 calculations within the framework of geometries optimized at the SCF level. To check the magnitude of the error introduced by this approach, the geometries of both the equilibrium complex (NCH...CN)<sup>-</sup> and the transition state (NC...H...CN)<sup>-</sup> were reoptimized at the MP2 level (holding the internal CN bond lengths fixed at their SCF values). Correlation was found to cause a contraction of the R(C...C) distance of 0.06 Å in the equilibrium complex, coupled with a stretch of the C-H bond of 0.02 Å. The geometry of the transition state was virtually unchanged by correlation which caused a very small stretch (0.01 Å) in R(C...C). The energetics are very little affected by these geometry reoptimizations: both the binding energy and the transfer barrier are increased by only 0.1 kcal/mol.

(31) Fowler, P. W.; Klein, M. L. *J. Chem. Phys.* **1986**, *85*, 3913.

(32) Szczesniak, M. M.; Scheiner, S. *J. Chem. Phys.* **1982**, *77*, 4586. Scheiner, S.; Harding, L. B. *J. Am. Chem. Soc.* **1981**, *103*, 2169; *J. Phys. Chem.* **1983**, *87*, 1145.

(33) Scheiner, S. *Acc. Chem. Res.* **1985**, *18*, 174.

(34) Scheiner, S. *J. Am. Chem. Soc.* **1981**, *103*, 315; *J. Chem. Phys.* **1982**, *77*, 4039; *J. Phys. Chem.* **1982**, *86*, 376. Scheiner, S.; Redfern, P. *Ibid.* **1986**, *90*, 2969.

(35) Hill, T. L. *Introduction to Statistical Thermodynamics*; Addison-Wesley: Reading, MA, 1960.

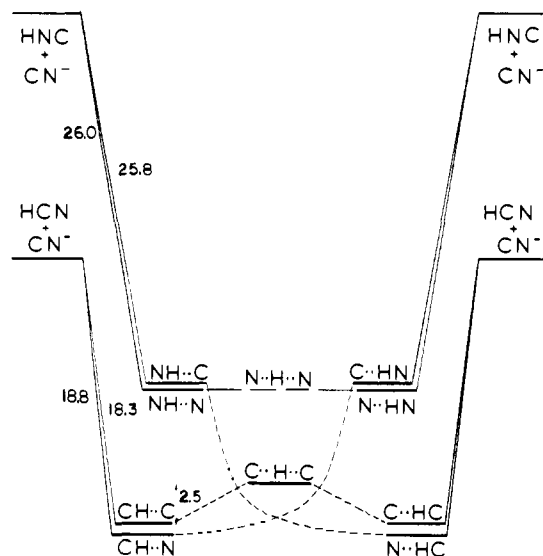


**Figure 1.** Energy profiles (kcal/mol) for reactions of  $\text{CN}^-$  with HCN or HNC. Notation for each complex includes only central H and atoms to which it is directly bonded. Broken lines indicate proton-transfer steps. After correction for ZPE, the transition state for proton transfer between N atoms in  $(\text{CN}\cdots\text{H}\cdots\text{NC})^-$  becomes lower in energy than the equilibrium  $(\text{CNH}\cdots\text{NC})^-$  complex.

**Vibrational Contributions.** The total zero-point vibrational energies (ZPE) of all the relevant species, calculated at the SCF level with the 6-31+G\*\* basis set, are listed in Table V, where the data displayed in the L = D column refer to the fully deuterated analogues. Comparison of the two columns of data reveals a fairly uniform trend: for all equilibrium structures, substitution of H with D lowers the ZPE by approximately 2 kcal/mol for each hydrogen present. For example, the ZPE of DCN is lower than that of HCN by 1.9 kcal/mol; the corresponding quantity for DCCD vs. HCCH is 3.8, while the ZPE of  $(\text{HC}\equiv\text{C}-\text{H}\cdots\text{C}\equiv\text{CH})^-$  is reduced by 5.7 kcal/mol when all three hydrogens are replaced by D. In all cases, the ZPE of the transition state to proton transfer ( $\text{A}\cdots\text{H}\cdots\text{B}$ ) is less than that of the equilibrium structure ( $\text{A}-\text{H}\cdots\text{B}$ ), leading to a lowering of the transfer barrier. This reduction lies within the range 2.5–2.8 kcal/mol for the protiated systems and 1.7–2.0 after deuteration. It is also generally true that the ZPE of a given equilibrium complex, e.g.,  $(\text{N}\equiv\text{C}-\text{H}\cdots\text{C}\equiv\text{N})^-$ , is greater (by ca. 1 kcal/mol) than the sum of the constituent subunits, in this case NCH and  $\text{CN}^-$ . Hence, consideration of vibrational energy would lower the binding energies reported in Table III by this amount. Of the various processes considered, the ZPE is most important in the protonation reactions of  $\text{CN}^-$  and  $\text{HCC}^-$ , reducing their protonation energies by between 7.9 and 8.6 kcal/mol (6.0–6.5 after deuteration).

Extension of the basis set would likely lead to only very small changes in the zero-point energies listed in Table V. For example, Lee and Schaefer<sup>26</sup> have computed near-Hartree-Fock limit frequencies for  $\text{HCC}^-$ , HCCH,  $\text{CN}^-$ , and HCN that are all within 2% of those calculated here with the 6-31+G\*\* basis set.

**Reaction Profiles.** The information in the preceding tables may be used to examine the energetics of the various pathways of the reaction between  $\text{CN}^-$  and either HCN or HNC in the gas phase. These pathways are traced in Figure 1 where association and dissociation reactions are indicated by solid lines and proton transfers by broken lines. The energy of each configuration is taken from our highest level of theory, MP2/6-31+G\*\*. The numeric labels in Figure 1 refer to the energy of the indicated association reaction (or in one case to the proton-transfer barrier) corrected by the zero-point vibrational energies reported in Table V. The energy scale is an absolute one: the separation between  $(\text{HNC} + \text{CN}^-)$  and  $(\text{HCN} + \text{CN}^-)$  on the left and right ends of the figure thus corresponds to the difference in energy between isomers HNC and HCN.

As indicated in Figure 1, HCN can initially form a H bond with either the C or N end of  $\text{CN}^-$ . At our highest level of theory,

these two possibilities are nearly isoenergetic with the  $\text{CH}\cdots\text{N}$  bond being favored by only 0.5 kcal/mol. If the  $(\text{NCH}\cdots\text{CN})^-$  complex is formed, the proton transfer between C atoms would pass through a transition state 2.5 kcal/mol higher in energy to form  $(\text{NC}\cdots\text{HCN})^-$  before dissociating to  $\text{NC}^-$  and HCN in an overall thermoneutral reaction. On the other hand, combined proton transfer and dissociation of the  $(\text{NCH}\cdots\text{NC})^-$  complex to  $\text{NC}^-$  and HNC is endothermic by 35.7 kcal/mol and would occur without passing directly through a  $(\text{NC}\cdots\text{HNC})^-$  intermediate since the latter structure is not a minimum in the MP2/6-31+G\*\* surface.

If  $\text{NC}^-$  is instead reacted with HNC, the energetically most likely pathway involves simultaneous complexation and proton transfer to form the  $(\text{CN}\cdots\text{HCN})^-$  complex, lower in energy than the reactants by 35.7 kcal/mol. Subsequent dissociation to HCN and  $\text{CN}^-$  requires 18.8 kcal/mol, with the overall two-step reaction exothermic by 16.9. The alternative is formation of a H bond to the N end of  $\text{CN}^-$  with  $(\text{CNH}\cdots\text{NC})^-$  more stable by 26.0 kcal/mol than the reactants. The transfer across the H bond to form  $(\text{CN}\cdots\text{HNC})^-$  occurs within a very flat potential with no effective barrier. The energetics of the deuterated systems are within 0.1 kcal/mol of the values presented in Figure 1; the only exception is the barrier for proton transfer in  $(\text{NC}-\text{D}\cdots\text{CN})^-$  which is 3.4 kcal/mol after correction for ZPE.

It should be noted that the lowest energy configuration in our potential-energy surface is  $(\text{NCH}\cdots\text{NC})^-$  which may appear at first sight surprising since the binding energy of this complex is only 18.8 kcal/mol, less than that of either complex in which HCN is replaced by HNC. The source of the lower *total* energy of  $(\text{NCH}\cdots\text{NC})^-$  is the presence of HCN, which although a weaker proton donor than HNC, and hence involved in weaker H bonds, is more stable than its isomer by 16.9 kcal/mol.

The SCF/6-31+G\*\* energetics are qualitatively similar with one major exception. Whereas there is no minimum in the MP2 surface corresponding to  $(\text{NC}\cdots\text{HNC})^-$ , this configuration is a true minimum in the SCF surface, separated from the more stable  $(\text{NCH}\cdots\text{NC})^-$  by a barrier of 2.7 kcal/mol. (On the other hand, this barrier is effectively neutralized by the smaller ZPE in  $(\text{NC}\cdots\text{H}\cdots\text{NC})^-$  as compared to  $(\text{NC}\cdots\text{H}-\text{NC})^-$ .) In fact, neglect of correlation leads to higher barriers separating all minima in the SCF surface.

The 4-31G reaction profiles are like SCF/6-31+G\*\* in that  $(\text{NC}\cdots\text{HNC})^-$  is separated from  $(\text{NCH}\cdots\text{NC})^-$  by a small energy barrier (here 1.1 kcal/mol which is again eliminated by inclusion of ZPE). The barriers in the symmetric systems are quantitatively similar to the MP2/6-31+G\*\* values. All levels of theory agree that the lowest energy structure in the potential energy surface of  $\text{CN}^-$  with either HCN or HNC is  $(\text{NCH}\cdots\text{NC})^-$ . However, whereas the larger set predicts  $(\text{NCH}\cdots\text{CN})^-$  to be quite close to this structure in energy, 4-31G erroneously places  $(\text{CNH}\cdots\text{NC})^-$  as second most stable, due in large part to the overestimate of the stability of HNC relative to HCN by this basis set.

The reaction profile of HCCH with  $\text{HCC}^-$  is symmetric in character and contains two equivalent minima at all levels of theory. At the MP2/6-31+G\*\* level,  $(\text{HCCH}\cdots\text{CCH})^-$  is lower in energy than the isolated subsystems by 9.7 kcal/mol and the energy barrier separating this structure from  $(\text{HCC}\cdots\text{HCCH})^-$  is 5.1 kcal/mol in height (5.9 for the deuterated analogue). Results calculated at lower levels of theory may be computed from the data in Tables III–V.

### Thermodynamic Properties

In the preceding sections, we have reported energetics of various processes at 0 K. However, since we have calculated all of the vibrational frequencies and geometries of the various complexes and monomers, it is also possible to use standard thermodynamic formulae<sup>35</sup> to evaluate  $\Delta H^\circ$ ,  $\Delta S^\circ$ , and  $\Delta G^\circ$  for the binding reactions over a range of temperatures. At 0 K,  $\Delta H^\circ$  is of course equal to  $\Delta E^\circ$ . As may be seen in the first section of Table VI,  $\Delta H^\circ$  remains nearly constant, changing by at most 1.7 kcal/mol over a 1000 K range of temperature. The less negative values of  $\Delta H^\circ$  at high temperature are due to the low-frequency vi-

**Table VI.** Thermodynamic Properties of Binding Reactions  $AH + B^- \rightarrow (AH \cdots B)^-$  Evaluated at Several Temperatures

	$\Delta H^\circ$ (kcal/mol)					
	1 K	10 K	100 K	300 K	500 K	1000 K
$(HCCH \cdots CCH)^-$	-9.73	-9.80	-10.07	-9.74	-9.32	-8.04
$(NCH \cdots CN)^-$	-18.29	-18.35	-18.71	-18.47	-18.07	-16.80
$(NCH \cdots NC)^-$	-18.82	-18.88	-19.22	-18.97	-18.58	-17.31
$(CNH \cdots CN)^-$	-25.85	-25.91	-26.31	-26.27	-26.10	-25.09
$(CNH \cdots NC)^-$	-25.98	-26.04	-26.40	-26.34	-26.16	-25.15
	$\Delta S^\circ$ (cal/K mol)					
	1 K	10 K	100 K	300 K	500 K	1000 K
$(HCCH \cdots CCH)^-$	1.64	-14.38	-24.63	-23.00	-21.93	-20.17
$(NCH \cdots CN)^-$	1.04	-14.98	-26.94	-25.84	-24.83	-23.09
$(NCH \cdots NC)^-$	0.80	-15.22	-26.69	-25.59	-24.59	-22.86
$(CNH \cdots CN)^-$	0.74	-15.27	-27.99	-27.90	-27.49	-26.14
$(CNH \cdots NC)^-$	0.52	-15.50	-27.49	-27.24	-26.82	-25.46
	$\Delta G^\circ$ (kcal/mol)					
	1 K	10 K	100 K	300 K	500 K	1000 K
$(HCCH \cdots CCH)^-$	-9.73	-9.65	-7.61	-2.84	1.65	12.14
$(NCH \cdots CN)^-$	-18.29	-18.20	-16.02	-10.72	-5.65	6.29
$(NCH \cdots NC)^-$	-18.82	-18.73	-16.55	-11.30	-6.28	5.55
$(CNH \cdots CN)^-$	-25.85	-25.76	-23.51	-17.90	-12.36	1.05
$(CNH \cdots NC)^-$	-25.98	-25.89	-23.65	-18.16	-12.76	0.31

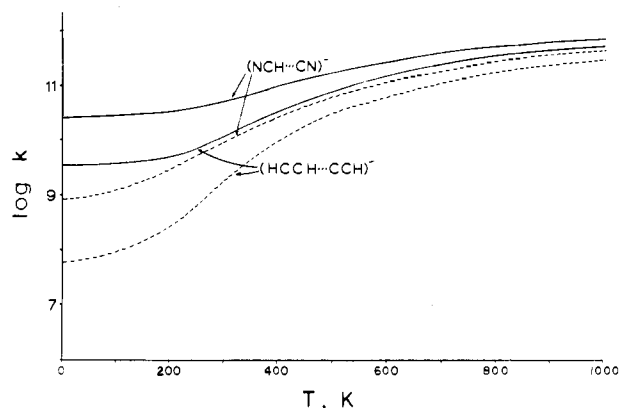
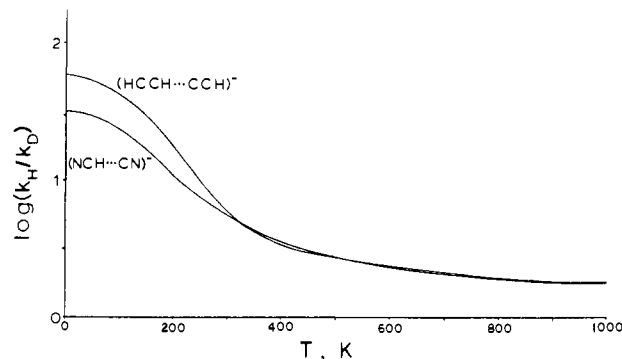
brations present in the  $(AH \cdots B)^-$  complexes, which may have their excited states increasingly populated as  $T$  rises. Note that the greatest temperature dependence occurs for the weakest complexes with which are associated the lowest frequency intermolecular vibrational modes.

Considering now the next section of data in Table VI, it may be seen that although  $\Delta S^\circ$  is approximately zero at 1 K, this property quickly becomes negative, even at very low temperatures, due primarily to the loss of translational and rotational degrees of freedom in going from a pair of reactants to a single complex. It may be noted that  $\Delta S^\circ$  is less negative for the weaker complexes, which may be ascribed to two different factors. First of all, the two subunits are further apart within the equilibrium geometries of the weaker complexes, leading to a larger moment of inertia and hence to greater rotational entropy. Second, weaker complexes have lower frequency intermolecular vibrations, allowing a broader distribution of vibrational quanta in the excited states, thereby resulting in more vibrational entropy.

The last section of Table VI reports the Gibbs free energies of binding which of course become increasingly positive at higher temperatures, due to the negative values of  $\Delta S^\circ$ . Thermoneutrality is reached at about 400 K for the complexation reaction of HCCH with  $CCH^-$ , occurs at about 750 K for the more strongly bound complexes of HCN with  $CN^-$ , and occurs at roughly 900 K for the still stronger complexation reaction of HNC. It is worth noting that the ordering of the five complexes by relative strength derived from the 0 K binding energies reported in Table III is identical with that determined by the criterion of either  $\Delta H^\circ$  or  $\Delta G^\circ$  and, moreover, remains constant over the full 1000 K range of temperature.

While the current literature contains no thermodynamic data for these complexes in the gas phase, Meot-Ner has very recently measured  $\Delta H^\circ$  and  $\Delta S^\circ$  for the binding of HCN with  $CN^-$  at a temperature of 400–500 K, obtaining values of  $-20.7 \pm 1.0$  kcal/mol and  $-21$  cal/(K·mol), respectively.<sup>36</sup> Although we cannot be sure whether the complex being formed is  $(NCH \cdots CN)^-$  or  $(NCH \cdots NC)^-$ , our calculations indicate the latter to be more likely. At 500 K, we would predict a value of  $\Delta H^\circ$  for this complex of  $-18.6$  kcal/mol, which is only 1 kcal/mol short of the experimental range. We consider this level of agreement quite encouraging, adding confidence to our other results. The remaining 1 or 2 kcal/mol likely resides in additional induction and dispersion attraction which would be accounted for by a larger and more flexible basis set, coupled with a more complete

(36) Meot-Ner, M., private communication.

**Figure 2.** Rate constant for proton transfer ( $s^{-1}$ ) calculated as a function of temperature. Broken curves refer to fully deuterated analogues.**Figure 3.** Deuterium isotope effect  $k_H/k_D$  (DIE).

treatment of electron correlation.

#### Proton-Transfer Rate

Of the systems considered here, it is only the proton transfer between C atoms in  $(NCH \cdots CN)^-$  and  $(HCCH \cdots CCH)^-$  for which there exists an energy barrier. We have calculated the rate of proton transfer in these two systems using the RRKM formalism,<sup>37</sup> within the context of the program written by Hase and Bunker,<sup>38</sup> adapted to include tunneling below the barrier according to Miller.<sup>39</sup> Boltzmann summation of the RRKM values leads to a canonical rate constant  $k(T)$ .<sup>40</sup> This procedure has been tested and compared to the Eyring formulation of transition-state theory in a number of prior works.<sup>39–41</sup>

The calculated rate constant is displayed as a function of temperature in Figure 2 for the  $(NCH \cdots CN)^-$  and  $(HCCH \cdots CCH)^-$  systems as well as their fully deuterated isotopomers (dashed curves). At temperatures below about 200 K, the rate of proton transfer in  $(NCH \cdots CN)^-$  is  $3 \times 10^{10} s^{-1}$  and nearly independent of  $T$ . This insensitivity is due to the dominating contribution of tunneling (essentially a temperature-independent process) to the rate at these low temperatures. As  $T$  is increased beyond 200 K, the population of higher energy states increases, the classical "over the barrier" transfer becomes more important, and the rate constant rises, approaching a high- $T$  asymptote of  $6 \times 10^{12} s^{-1}$ . The  $(HCCH \cdots CCH)^-$  system behaves in a similar manner, although exhibiting a slightly greater sensitivity to  $T$ , varying from  $4 \times 10^9 s^{-1}$  at 0 K to  $5 \times 10^{12} s^{-1}$  at infinite temperature. This greater sensitivity, as well as the slower rate of transfer at any value of  $T$ , is due to the slightly higher transfer barrier of 7.6 kcal/mol in  $(HCCH \cdots CCH)^-$  as compared to 5.3 for  $(NCH \cdots C-N)^-$ .

(37) Robinson, P. J.; Holbrook, K. A. *Unimolecular Reactions*; Wiley-Interscience: New York, 1972. Forst, W. *Theory of Unimolecular Reactions*; Academic Press: New York, 1973. Hase, W. L. *Acc. Chem. Res.* **1983**, *16*, 258.(38) Hase, W. L.; Bunker, D. L. *QCPE* **1973**, *11*, 234.(39) Miller, W. H. *J. Am. Chem. Soc.* **1979**, *101*, 6810.(40) Scheiner, S.; Latajka, Z. *J. Phys. Chem.* **1987**, *91*, 724.(41) Hayashi, S.; Umamura, J.; Kato, S.; Morokuma, K. *J. Phys. Chem.* **1984**, *88*, 1330.

The dashed curves in Figure 2 represent the transfer rates in the deuteriated systems  $(\text{NCD}\cdots\text{CN})^-$  and  $(\text{DCCD}\cdots\text{CCD})^-$ . Although comparable to the rates of the undeuteriated analogues at high temperature, the transfer becomes notably slower as  $T$  is diminished. This slowdown is due in large part to the greater importance assumed by the tunneling process at lower temperatures: the heavier D nucleus tunnels much less rapidly than does the proton. The ratio of  $k_{\text{H}}/k_{\text{D}}$ , also known as the deuterium isotope effect (DIE), is illustrated for both systems as a function of  $T$  in Figure 3. The DIE is fairly small at high temperatures, approaching 1.4 and 1.5 for the  $(\text{NCH}\cdots\text{CN})^-$  and  $(\text{HCCH}\cdots\text{CCH})^-$  systems, respectively, as  $T \rightarrow \infty$ . The DIE rises as the temperature is diminished, attaining a value of 6 at 300 K. Below this temperature, the DIEs of the two systems diverge from one another with both flattening out below 50 K. The low-temperature limit of the DIE for  $(\text{NCH}\cdots\text{CN})^-$  is 30 while that for  $(\text{HCCH}\cdots\text{CCH})^-$ , with its slightly higher transfer barrier, is 60. "Plateau" behavior of this type, with similarly high values of the DIE, has been observed experimentally in a number of prior cases.<sup>40,42,43</sup>

In a previous study of  $(\text{H}_3\text{CH}\cdots\text{CH}_3)^-$ , it was demonstrated that tunneling plays a dominant role in the proton-transfer process at low and intermediate temperatures.<sup>40</sup> Taking 300 K as a sample temperature, the rate constant calculated with tunneling excluded was found smaller by a factor of 10 than the correct value of  $k$ ; this factor becomes progressively larger as the temperature is diminished. Since the transfer barriers of the two systems being considered here are substantially lower than the barrier of 15.4 kcal/mol in  $(\text{H}_3\text{CH}\cdots\text{CH}_3)^-$ , it is reasonable to presume that tunneling will be less important. This was indeed found to be the case. Whereas the rate constants calculated with and without tunneling for  $(\text{H}_3\text{CH}\cdots\text{CH}_3)^-$  diverge at temperatures below 500 K, the onset of this separation, where tunneling begins to make a substantial contribution, is pushed down to 400 K for both  $(\text{NCH}\cdots\text{CN})^-$  and  $(\text{HCCH}\cdots\text{CCH})^-$ . Ignoring the possibility of tunneling leads to an underestimate of  $k$  by a factor of 2 for the latter systems at 300 K, as compared to 10 for  $(\text{H}_3\text{CH}\cdots\text{CH}_3)^-$ . Nevertheless, even in these systems with their lower barriers, tunneling is the major mechanism of proton transfer at lower temperatures, overshadowing the classical process by many orders of magnitude.

Our earlier calculations<sup>40</sup> have demonstrated the sensitivity of the transfer rate constant to the precise height of the energy barrier. Needless to say, our calculated barriers do not represent the last word as they could conceivably be improved by using larger basis sets and more complete treatments of correlation. There is thus some margin of error in the quantitative aspects of Figures 2 and 3; however, the dominating influence of tunneling at low temperatures is essentially invariant to application of higher levels of theory, as are the qualitative trends in these figures.

### Uniform H-Bond Length

Inspection of Table II reveals that the distances between the two subunits in the various complexes are quite different from one another; the same is true regarding the transition states for proton transfer. Since transfer energetics are quite sensitive to the distance between the two groups within a H bond,<sup>32-34</sup> this variation represents an additional layer of complexity that must be unraveled in analyzing the dependence of the energetics upon the fundamental properties of the systems involved. In principle, a more uniform framework for comparison would be provided by studying all the systems at a single fixed H-bond length.

From another perspective, the calculations described above have been concerned with association of the  $\text{CN}^-$  and  $\text{HCC}^-$  ions with the  $\text{HCN}$ ,  $\text{HNC}$ , and  $\text{HCCH}$  molecules in the gas phase where

**Table VII.** Energy Barriers to Proton Transfer (kcal/mol) from Left to Right for Fixed H-Bond Length  $R(\text{X}\cdots\text{Y}) = 2.95 \text{ \AA}$  ( $\text{X}, \text{Y} = \text{C}, \text{N}$ )

	MP2/ 6-31+G**	SCF/ 6-31+G**	SCF/ 4-31G
$(\text{HCCH}\cdots\text{CCH})^-$	7.0	11.6	8.9
$(\text{NCH}\cdots\text{CN})^-$	6.5	10.5	8.4
$(\text{CNH}\cdots\text{NC})^-$	12.3	20.0	16.5
$(\text{NCH}\cdots\text{NC})^-$	14.6	19.0	14.4
$(\text{CNH}\cdots\text{CN})^-$	4.1	10.7	9.5

the complexes are subject to no geometrical constraints and can consequently adopt their energetically most favorable configurations. On the other hand, when the two groups comprise an intramolecular H bond within a single large molecule, their separation is determined to a large extent by the structural constraints imposed by the macromolecular skeleton.<sup>44</sup> Nor would the optimum geometry be expected in solution where solvent molecules can impose additional spatial restrictions on the H-bonded pair.

We therefore proceed as follows. An intermolecular separation  $R(\text{X}\cdots\text{Y})$  is chosen (where X and Y represent the C or N atoms participating in the H bond) and held fixed as the proton is transferred between the two subunits. All geometrical parameters, except for this single distance, are fully optimized for both wells in the transfer potential  $(\text{XH}\cdots\text{Y})$  and  $(\text{X}\cdots\text{HY})$  as well as the transition state separating them  $(\text{X}\cdots\text{H}\cdots\text{Y})$ . The proton-transfer barriers computed for  $R = 2.95 \text{ \AA}$  are reported in Table VII for each of our different systems. A trend repeated here for fixed  $R$ , as noted above when  $R$  was allowed to change during the transfer, is the increase in barrier height associated with enlargement of the basis set and the barrier reduction arising from correlation. At any level of theory, the systems fall into one of two categories: in those cases in which the proton is transferred toward a C atom, the barrier is notably lower than when a N atom acts as acceptor. As a corollary, the barrier for transfer between two N atoms is appreciably higher than that for intercarbon transfer.

The effects of correlation are not uniform from one system to the next, leading to some interesting trend reversals. For example, at the SCF level, the barrier for  $(\text{CNH}\cdots\text{CN})^-$  is predicted to be slightly higher than that of  $(\text{NCH}\cdots\text{CN})^-$  whereas the barrier of the former system is significantly smaller at the MP2 level. A similar reversal is observed between  $(\text{CNH}\cdots\text{NC})^-$  and  $(\text{NCH}\cdots\text{NC})^-$ . It thus appears that inclusion of correlation is necessary in order to correctly assess the relative barrier heights within these subsets of systems.

It was noted earlier that when  $R$  is included in the optimization, the SCF/4-31G scheme furnished transfer barriers for the symmetric systems in generally satisfactory agreement with the MP2/6-31+G\*\* procedure (see Table IV). This level of agreement deteriorates, however, when  $R$  is held constant during the transfer, as may be seen by a comparison of the first and third columns of data in Table VII. The SCF/4-31G barriers are significantly overestimated in all cases, with the exception of  $(\text{NCH}\cdots\text{NC})^-$  where this tendency of 4-31G is compensated by the basis set's aforementioned exaggeration of the proton affinity of the N end of  $\text{CN}^-$ . Transfer barriers were also computed for several other values of  $R$  in addition to 2.95 Å. A rapid increase in barrier height is caused by elongation of the H bond, conforming to principles elucidated previously for a variety of other systems.<sup>33,34</sup> Whereas SCF/4-31G may overestimate the transfer barriers, the functional dependence of this quantity upon  $R$  closely parallels the more accurate MP2/6-31+G\*\* data.

It is important to note that whereas our earlier data in Table IV had suggested higher barriers for proton transfer between C

(42) Brunton, G.; Griller, D.; Barclay, L. R. C.; Ingold, K. U. *J. Am. Chem. Soc.* **1976**, *98*, 6803. Brunton, G.; Gray, J. A.; Griller, D.; Barclay, L. R. C.; Ingold, K. U. *J. Am. Chem. Soc.* **1978**, *100*, 4197. Grellman, K.-H.; Weller, H.; Tauer, E. *Chem. Phys. Lett.* **1983**, *95*, 195. Grellman, K. H.; Schmitt, U.; Weller, H. *Ibid.* **1982**, *88*, 40.

(43) Tokumura, K.; Watanabe, Y.; Itoh, M. *J. Phys. Chem.* **1986**, *90*, 2362. Bromberg, A.; Muskat, K. A.; Fischer, E.; Klein, F. S. *J. Chem. Soc., Perkin Trans. 2* **1972**, 588.

(44) Baker, E. N.; Hubbard, R. E. *Prog. Biophys. Mol. Biol.* **1984**, *44*, 97. Houriet, R.; Rüfenacht, H.; Carrupt, P.-A.; Vogel, P.; Tichy, M. *J. Am. Chem. Soc.* **1983**, *105*, 3417. Olovsson, I.; Jönsson, P.-G. In *The Hydrogen Bond—Recent Developments in Theory and Experiments*; Schuster, P., Zundel, G., Sandorfy, C., Eds.; North-Holland: Amsterdam, 1976.

atoms than for internitrogen transfer, the situation is reversed when all three systems are restricted to the same value of  $R$ , as shown in the first column of Table VII. It is therefore apparent that one must carefully define the problem when considering the question as to which system has associated with it the fastest transfer (lowest barrier). Transfers between a pair of carbon atoms are intrinsically *faster* than internitrogen transfer, *provided* there are similar intersubunit separations in the two systems. The barriers in both types of systems increase quickly as the two groups are moved further from one another. The slower transfer observed between C atoms when the length of the H bond is unconstrained is hence due to the much longer equilibrium separation between the C atoms, which is, in turn, a result of the weaker H bond.

A similar principle can be used in a comparison of the two intercarbon transfers. We see from Table VII that the *intrinsic* barrier (same  $R$ ) for  $(\text{HCCH}\cdots\text{CCH})^-$  is only slightly higher than that for  $(\text{NCH}\cdots\text{CN})^-$ , the small difference being due perhaps to the shorter  $r(\text{CH})$  in  $\text{HCCH}$ .<sup>33,45</sup> The larger barrier difference in Table IV arises primarily because of the weaker H bond in  $(\text{HCCH}\cdots\text{CCH})^-$  and its associated longer intermolecular separation  $R(\text{C}\cdots\text{C})$ .

A final distinction along these lines concerns the manner in which the transfer barrier is affected by the identity of the two subunits. As may be seen in Table IV wherein  $R$  is included in the optimization, the barrier is most sensitive to the nature of the proton-donor molecule with the acceptor playing a less important role. That is, the lowest barriers occur when the more acidic HNC acts as proton donor, regardless of the identity of the acceptor. In contrast, when  $R$  is restricted to a uniform value for all systems, it is the identity of the proton *acceptor* that becomes the decisive factor. As indicated in Table VII, the barriers are raised by only 2 kcal/mol when the HNC proton donor is replaced by the less acidic HCN whereas changing the proton acceptor from the C end of  $\text{CN}^-$  to the less basic N end causes an enlargement of 8 kcal/mol.

### Summary and Discussion

The calculations described above have provided evidence that the potential energy surfaces pertinent to proton transfer between C atoms in  $(\text{NCH}\cdots\text{CN})^-$  and  $(\text{HCCH}\cdots\text{CCH})^-$  each contain a pair of equivalent minima separated by an energy barrier. In contrast, the transfer between two electronegative atoms, such as the  $(\text{CNH}\cdots\text{NC})^-$  studied here or other H-bonded systems examined previously,<sup>32-34,45</sup> characteristically occurs in the absence of any such barrier. These results therefore support the prior assertion of a higher barrier for transfers between C atoms.

The data reported here also offer an explanation of the experimental observation<sup>3</sup> that HCN behaves in a manner inter-

mediate between other carbon acids and "normal" acids, i.e., those involving electronegative atoms O or N. Gas-phase proton transfer occurs without a barrier between the latter electronegative atoms, while transfers between C acids are generally characterized by barriers in excess of 10 kcal/mol.<sup>46</sup> The proton transfer potential in  $(\text{NCH}\cdots\text{CN})^-$  is intermediate between these two extremes: although it contains two wells like other C acids, the barrier separating the two minima is quite small, only about 2.5 kcal/mol after correction for vibrational motions.

In addition, our calculations have allowed us to unambiguously attribute the transfer barriers associated with C acids to the longer equilibrium separation between the two C atoms involved in the proton transfer, as compared to the internuclear distances in H bonds involving O or N. In fact, when the various types of H bonds are constrained to similar lengths, transfer barriers between carbon atoms are of *lesser* height than those involving more electronegative atoms. These observations extend our earlier findings<sup>32-34</sup> which may be summarized as follows. Under the constraint of a uniform fixed H-bond length  $R(\text{XX})$ , proton-transfer barriers diminish as the electronegativity of X decreases. This trend appears to be tied to an elongation of the equilibrium X-H bond in the monomer as X becomes less electronegative, i.e.,  $r(\text{OH}) < r(\text{NH}) < r(\text{CH})$ .<sup>33,45</sup> A longer X-H bond lessens the distance the proton must traverse toward the X $\cdots$ X midpoint where the transition state occurs, hence lowering the barrier. However, this rule is counteracted by an opposing pattern when the restriction of fixed  $R(\text{XX})$  is lifted because this same progression from O to N to C leads to weaker, and hence longer, equilibrium H-bond lengths. This stretch in  $R(\text{XX})$  far outweighs the associated elongation of  $r(\text{XH})$  and the proton must hence traverse a much greater distance to the X $\cdots$ X midpoint, leading to the observed increase in the "effective" barrier.

In sum, the *intrinsic* proton-transfer barrier, i.e., uniform H-bond length  $R$ , is most sensitive to the nature of the proton-acceptor group, with the barrier diminishing as this group becomes more basic. The situation is reversed, on the other hand, when the intermolecular distance is freed of external constraint since the strength of the H bond is dominated by the identity of the proton *donor* group. A more acidic donor better attracts the acceptor, contracting the H bond and lowering the barrier by allowing the proton to move a shorter distance.

**Acknowledgment.** We are grateful to Dr. Z. Latajka for assistance with some of the computations and to Dr. M. Meot-Ner for communicating to us his measurements prior to publication. Some of the calculations were carried out on the SIU Theoretical Chemistry Computer, funded in part by a grant from the Harris Corp. This work was supported by grants from the National Institutes of Health (GM29391 and AM01059) and from the National Science Foundation (DMB-8612768).

(45) Hillenbrand, E. A.; Scheiner, S. *J. Am. Chem. Soc.* **1985**, *107*, 7690; **1984**, *106*, 6266; **1986**, *108*, 7178. Scheiner, S.; Hillenbrand, E. A. *J. Phys. Chem.* **1985**, *89*, 3053.

(46) Latajka, Z.; Scheiner, S. *Int. J. Quantum Chem.* **1986**, *29*, 285.